



# Melt electrospinning of daunorubicin hydrochloride-loaded poly ( $\epsilon$ -caprolactone) fibrous membrane for tumor therapy



He Lian, Zhaoxu Meng\*

Department of Biomedical Engineering, School of Medical Devices, Shenyang Pharmaceutical University, Shenyang, 110016, China

## ARTICLE INFO

### Article history:

Received 30 November 2016

Accepted 19 March 2017

Available online 6 April 2017

### Keywords:

Melt electrospinning

Drug delivery system

Poly ( $\epsilon$ -caprolactone)

Daunorubicin hydrochloride

Tumor therapy

## ABSTRACT

Daunorubicin hydrochloride is a cell-cycle non-specific antitumor drug with a high therapeutic effect. The present study outlines the fabrication of daunorubicin hydrochloride-loaded poly ( $\epsilon$ -caprolactone) (PCL) fibrous membranes by melt electrospinning for potential application in localized tumor therapy. The diameters of the drug-loaded fibers prepared with varying concentrations of daunorubicin hydrochloride (1, 5, and 10 wt%) were  $2.48 \pm 1.25$ ,  $2.51 \pm 0.78$ , and  $2.49 \pm 1.58$   $\mu\text{m}$ , respectively. Fluorescence images indicated that the hydrophobic drug was dispersed in the hydrophilic PCL fibers in their aggregated state. The drug release profiles of the drug-loaded PCL melt electrospun fibrous membranes were approximately linear, with slow release rates and long-term release periods, and no observed burst release. The MTT assay was used to examine the cytotoxic effect of the released daunorubicin hydrochloride on HeLa and glioma cells (U87) *in vitro*. The inhibition ratios of HeLa and glioma cells following treatment with membranes prepared with 1, 5, and 10 wt% daunorubicin hydrochloride were 62.69%, 76.12%, and 85.07% and 62.50%, 77.27%, and 84.66%, respectively. Therefore, PCL melt electrospun fibrous membranes loaded with daunorubicin hydrochloride may be used in the local administration of oncotherapy.

© 2017 The Authors. Production and hosting by Elsevier B.V. on behalf of KeAi Communications Co., Ltd. This is an open access article under the CC BY-NC-ND license (<http://creativecommons.org/licenses/by-nc-nd/4.0/>).

## 1. Introduction

In recent years, the global incidence of cancer has steadily increased. Therefore, considerable efforts have been made in the improvement of the therapeutic options and treatments of cancer. An effective treatment can prevent postoperative tumor recurrence and enhance the survival and quality of life of patients. Thus far, radiotherapy and chemotherapy remain the main clinical treatment options [1–4]. Chemotherapeutic drugs have an inherently high cytotoxicity, and therefore their oral or intravenous administration leads to organ damage, including hepatotoxicity and nephrotoxicity, decreasing the patient's health and quality of life [5,6]. Local administration is an effective method to reduce chemotherapeutic toxicity by placing the drug directly in the tumor resection site, which does not only remove residual tumor cells and prevent tumor recurrence, but also reduces systemic damage of the drug to normal cells. The key issue to achieving local chemotherapy

administration is the development of suitable drug delivery systems (DDS) with long-term drug release profiles that simultaneously promote tissue repair. Several local administration DDS have been developed, including micelles, hydrogels, and nanoparticles; however, control of their burst release profiles and low drug loading remains a challenge [7–10].

Electrospinning is a method to fabricate ultrafine fibers with diameters ranging from the micro to the nano scale. Recently, fibers prepared through electrospinning have been widely applied in the biomedical field, including as tissue engineering scaffolds, as drug carriers, and in wound repair. The great success of these materials is due to the combination of inorganic and organic components as raw materials and the similarity of their physical properties to those of the extracellular matrix, namely a large surface to volume ratio, a high porosity, and an interconnected pore structure [11–14]. Therefore, compared to other drug carriers, electrospun fibers can promote tissue regeneration [15,16]. Nevertheless, drug loading in electrospun fibers is often limited by the solubility of the drug and the solvent concentration in the mixed solvent system.

Herein, we developed a DDS via a solvent-free melt

\* Corresponding author.

E-mail address: [mengzhaoxu2006@163.com](mailto:mengzhaoxu2006@163.com) (Z. Meng).

Peer review under responsibility of KeAi Communications Co., Ltd.

electrospinning method in order to address the solvent limitation issues [17–19]. Poly ( $\epsilon$ -caprolactone) (PCL) was selected as the drug carrier due to its low melting point (about 60 °C) and its suitability in the melt encapsulation of several drugs [20,21]. Furthermore, the long degradation time of PCL makes it suitable for long-term drug release. Daunorubicin hydrochloride was chosen as the model drug due to its excellent fluorescence properties, allowing observation of its dispersion within the matrix.

## 2. Materials and methods

### 2.1. Materials

Poly ( $\epsilon$ -caprolactone) ( $M_w = 40,000$ ) was a commercial product from Shenzhen Polymtek Bomaterial Co. Ltd. (China). Daunorubicin hydrochloride (CAS: 23541-50-6, particle size: 0.1–0.8  $\mu\text{m}$ ) were purchased from Dalian Meilun Biology Technology Co. Ltd. (China). All the other chemicals were of analytical reagent grade and used without further purification.

### 2.2. Melt electrospinning

PCL was heated into a melt at 90 °C with a self-made electrical heater. Subsequently, daunorubicin hydrochloride was added into the PCL melt and stirred by mechanical agitation until the melt color became a uniform red; three daunorubicin hydrochloride mixtures were prepared, with drug concentrations of 1, 5, and 10% by weight, respectively. The melt was then transferred to a heated syringe to maintain the temperature at 90 °C. When a voltage of +30 kV was applied to the melt, the melt jet was formed and collected on the metal plate, placed on the front of the syringe at a distance of 15 cm; the melt flow rate was set to 1.5 mL/h.

### 2.3. Characterization

The fiber morphology was characterized by scanning electron microscopy (SEM) at an accelerating voltage of 15 kV. All samples were dried under a vacuum prior to coating with a thin layer of gold. The diameters of the resulting fibers were analyzed using software Image J. The fluorescence of the drug-loaded fibers was characterized by fluorescence microscopy (Olympus BX53, Japan). FT-IR spectra of the drug-loaded fibrous membranes were recorded in the ATR mode with an IR spectrophotometer (Nicolet iS5, USA) within the 4000–400  $\text{cm}^{-1}$  range. X-ray diffraction analysis was performed using an X-ray diffractometer (Bruker D8 Advance, Germany) equipped with a Cu-K $\alpha$  source, operating at 40 kV and 100 mA.

### 2.4. Drug release

Drug-loaded samples were dissolved in dichloromethane and the drug was extracted in PBS. The actual drug content was measured via UV–Vis spectrometry ( $\lambda = 490 \text{ nm}$ ) and calculated using a predetermined drug calibration curve. To evaluate the drug release profile of the drug-loaded fibrous membranes, 2 g of the drug-loaded sample were transferred to a flask containing 1000 mL of PBS (pH 7.4) and stirred with a magnetic stirrer at 100 rpm and 37 °C. At various time points, 2 mL of the release medium were retrieved and replaced by fresh PBS. The amount of released drug was determined by UV–vis spectrophotometry.

### 2.5. Cytotoxicity

Two tumor cell lines (HeLa cells and glioma cells (U87)) were selected as model cells to assess the cytotoxicity of the drug-loaded

PCL melt electrospun fibrous membrane. HeLa cells were cultured in H-DMEM, supplemented with 10% FBS, 100 U/mL penicillin, and 100  $\mu\text{g}/\text{mL}$  streptomycin in a normal  $\text{CO}_2$  incubator at 37 °C. U87 cells were cultured in L-DMEM containing 10% FBS, 100 U/mL penicillin, and 100  $\mu\text{g}/\text{mL}$  streptomycin at 37 °C and 5%  $\text{CO}_2$ . When cells reached 80–90% confluence, they were trypsinized and counted with a hemocytometer.

The drug-loaded PCL melt electrospun fibrous membranes were cut into small pieces of equal weight (5 mg) and placed at the bottom of 24-well plates, followed by sterilization under UV radiation for 12 h. Subsequently, cells were added to each well at a density of  $1 \times 10^6$  cells/mL in 2 mL of medium per well and cultured in a humidified atmosphere with 5%  $\text{CO}_2$  at 37 °C. The culture medium was refreshed every 2 days using a medium simultaneously incubated with the drug-loaded sample (5 mg/mL) in order to maintain the concentration of released drug at the corresponding time point.

For MTT assay, the cells were incubated in MTT (5 mg/mL) for 4 h in 5%  $\text{CO}_2$  at 37 °C. Then, 100  $\mu\text{L}$  of sodium dodecyl sulfate (10 wt% SDS in 0.01 M HCl) were added to each well and incubated for 24 h to dissolve the internalized purple formazan crystals. The absorbance was measured at 570 nm with a reference wavelength of 630 nm using a microplate reader (Bio-RAD680, Bio-rad Co., USA).

### 2.6. Statistical analysis

Origin 8.0 (Origin Lab Inc., USA) software was used to analyze the obtained data. One-way Analysis of Variance (ANOVA) was employed for the statistical analysis of the data. All measurements were performed in triplicate and all values were expressed as means  $\pm$  standard deviation (SD).

## 3. Results and discussion

### 3.1. Morphology

The morphologies of the drug-loaded fibers are shown in Fig. 1. Most fibers appeared curled, demonstrating the typical morphology of melt electrospun fibers following solidification and condensation from the melt jet [20,22]. Moreover, the fiber diameters were  $2.48 \pm 1.25$ ,  $2.51 \pm 0.78$ , and  $2.49 \pm 1.58 \mu\text{m}$  for the 1, 5, and 10 wt% drug-loaded samples. Thus, the fiber diameters remained largely unchanged, likely due to the high viscosity of the melt decreasing the influence of the drug on the spinning process [23]. In addition, the fiber surfaces were smooth without the appearance of drug crystals or other impurities, indicating that the drug was encapsulated inside the fiber.

### 3.2. Fluorescence

Due to the high fluorescence of daunorubicin hydrochloride, the dispersion of the drug was clearly observed through fluorescence microscopy (Fig. 2). The fluorescence intensity increased with increasing drug content, with extensive bright spots throughout the fiber, demonstrating that, although the drug was encapsulated inside the melt electrospun fiber, the dispersion was not uniform. The lack of uniform dispersion may be attributed to repulsion between the hydrophilic drug and the hydrophobic PCL matrix, leading to the aggregation of drugs within the fibers.

### 3.3. FT-IR

The FT-IR spectra of the samples are shown in Fig. 3. Characteristic peaks at 2949  $\text{cm}^{-1}$ , 2865  $\text{cm}^{-1}$ , 1727  $\text{cm}^{-1}$ , 1297  $\text{cm}^{-1}$ , 1245  $\text{cm}^{-1}$ , and 1190  $\text{cm}^{-1}$  were observed for PCL, corresponding to

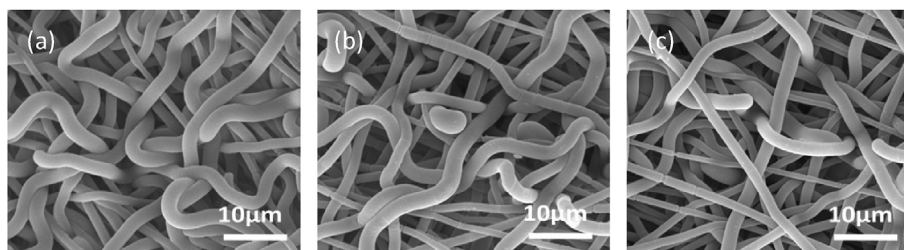


Fig. 1. SEM images of PCL melt electrospun fibers containing daurorubicin hydrochloride at (a) 1 wt%, (b) 5 wt%, and (c) 10 wt%.

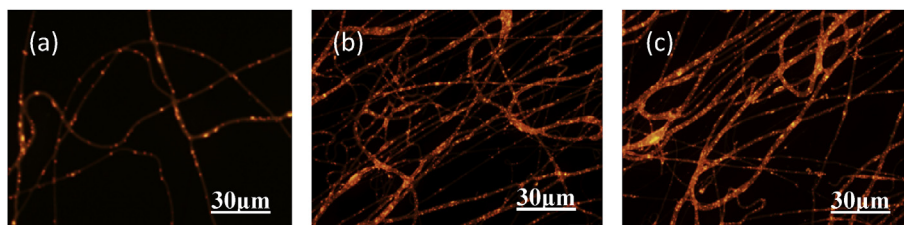


Fig. 2. Fluorescence images of PCL melt electrospun fibers containing daurorubicin hydrochloride at (a) 1 wt%, (b) 5 wt%, and (c) 10 wt%.

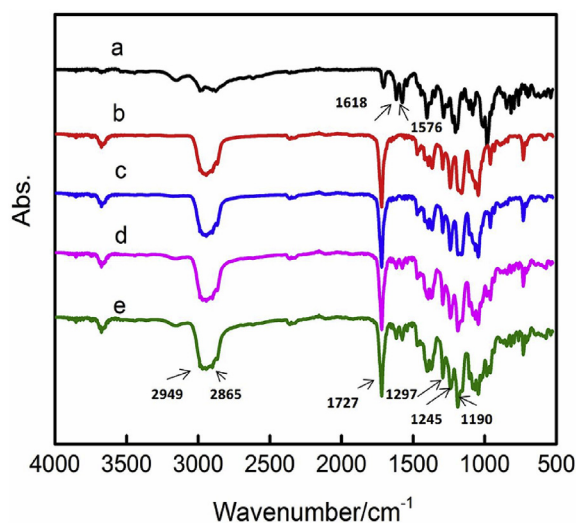


Fig. 3. FT-IR spectra of (a) daurorubicin hydrochloride, (b) pure PCL melt electrospun fiber, and (c–e) PCL melt electrospun fibers containing daurorubicin hydrochloride at (c) 1 wt%, (d) 5 wt%, and (e) 10 wt%.

the asymmetric  $\text{CH}_2$  stretching, symmetric  $\text{CH}_2$  stretching, carbonyl stretching, C–O and C–C stretching in the crystalline phase, asymmetric C–O–C stretching, and OC–O stretching vibrations, respectively [24]. Two characteristic peaks belonging to daurorubicin hydrochloride at  $1618\text{ cm}^{-1}$  and  $1576\text{ cm}^{-1}$ , assigned to the stretching of hydrogen-bonded quinone carbonyl groups and C=C stretching vibrations, respectively, were observed in the spectrum of daurorubicin hydrochloride-loaded PCL melt fibers [25]. Moreover, the peaks assigned to daurorubicin hydrochloride and PCL were not observed to shift with changes in drug content, further indicating a lack of interaction between the drug molecules and PCL.

#### 3.4. In vitro drug release and cytotoxicity

As a DDS for the local administration of tumor therapy, maintaining a relatively stable drug concentration at the focus of the

lesion is of great significance to the removal of residual tumor cells. Thus, the drug release rate and sustained release time are important factors of the DDS. Table 1 shows that the drug loading efficiency of the fibers was above 95% for all three drug concentrations, with the values decreasing with increasing drug content. This is likely due to high drug concentrations leading to an increase in drug aggregation, resulting in a lack of uniform dispersion of the drug within the PCL fibers.

Fig. 4 depicts the release profiles of daurorubicin hydrochloride from PCL melt electrospun fibers at the various drug concentrations. The release rate profiles show a two-stage process, wherein there is a slow release during the initial 3–4 days, subsequently followed by a slightly higher release rate; this phenomenon was more obvious with the increasing drug content.

During melt electrospinning, fibers are formed by the cooling and solidification of the melt jet, and therefore crystals may form through rearrangement of the molecular chains of PCL [23,26]. Indeed, XRD analysis (Fig. S1 in SI) confirmed that the crystallinity of the PCL melt electrospun fibers was similar to that of pure PCL. In this case, the high degree of crystallization and the hydrophobicity of the PCL melt electrospun fiber inhibited the penetration of water and the diffusion of the drug, thereby avoiding a burst drug release. However, after a period of time, water was able to diffuse within the fibers through the amorphous regions due to the loose arrangement of the molecular chains, thereby releasing a large amount of drug [26,27]. Thus, this is observed by the turning point in the drug release curve, and was more obvious with increasing drug content. In addition, the drug-loaded PCL melt electrospun fibers showed potential as long-term DDS considering that the drug release ratio was only 20% after 2 weeks, even when the drug content in the fiber was up to 10 wt%.

Two tumor cell lines (HeLa and glioma (U87) cells) were

Table 1  
Drug-loading efficiency of PCL melt electrospun fibrous membranes.

Samples	Loading efficiency (%)
PCL-1 wt% drug	$99.68 \pm 0.45$
PCL-5 wt% drug	$96.03 \pm 3.98$
PCL-10 wt% drug	$95.76 \pm 4.55$

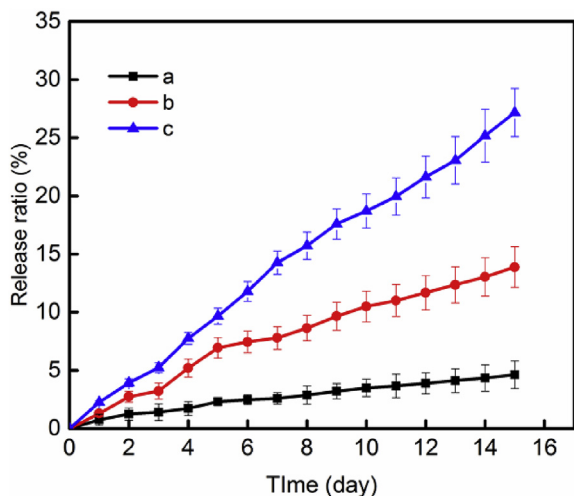


Fig. 4. Release profiles of PCL melt electrospun fiber containing with daurorubicin hydrochloride at (a) 1 wt%, (b) 5 wt% and (c) 10 wt%.

cultured on the surface of the various drug-loaded PCL melt electrospun fibers and assessed by the MTT assay in order to detect the cytotoxicity of the fibers (Fig. 5). The drug-loaded PCL melt

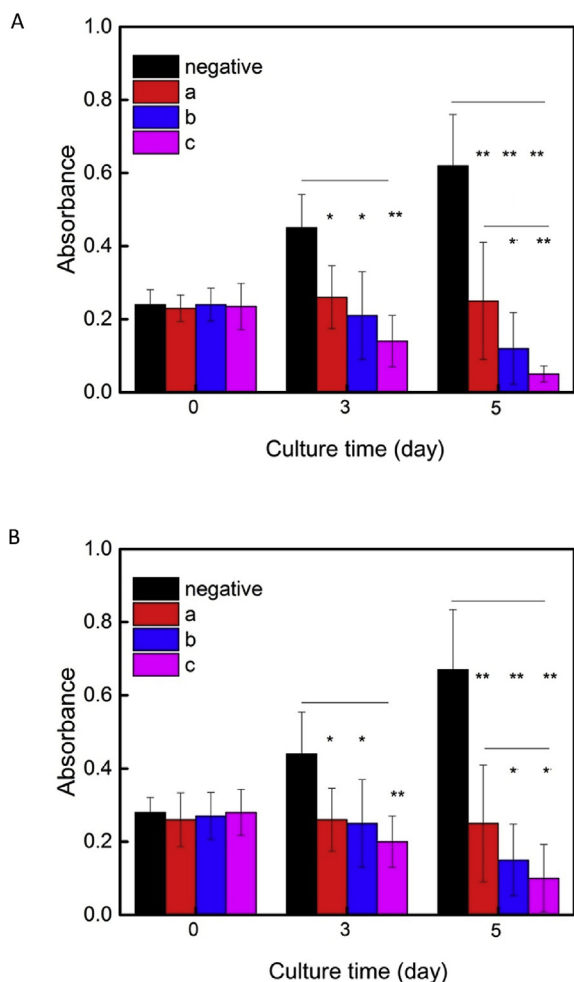


Fig. 5. MTT assay of HeLa (A) and U87 (B) cell survival following treatment with PCL melt electrospun fibers containing daurorubicin hydrochloride at (a) 1 wt%, (b) 5 wt%, and (c) 10 wt% (\* $P < 0.05$ , \*\* $P < 0.01$ ).

electrospun fibers exhibited excellent antitumor properties, significantly inhibiting tumor cell growth, with the effect increasing with increasing drug content. Daunorubicin hydrochloride was selected as a model hydrophilic drug, although several other antitumor drugs could also be embedded within the PCL melt electrospun fiber.

#### 4. Conclusions

In summary, daunorubicin hydrochloride-loaded PCL fibrous membranes were fabricated by melt electrospinning as an anti-tumor DDS for the local administration of tumor therapy. The fibers had a smooth morphology, with the hydrophobic drug almost completely encapsulated within the fiber, although aggregation of the drug increased with increasing drug content. Melt electrospinning enhances the crystallization of the drug-loaded PCL fibrous membranes, resulting in a slow drug release rate and a long-term release period. The drug-loaded PCL fibrous membrane also exhibited an excellent effect on the inhibition of tumor cell growth. Therefore, PCL melt electrospun fibers may be a potential candidate for long-term DDS in the local administration of tumor therapy.

#### Acknowledgement

This work is supported by the Scientific Research General Project of Liaoning Provincial Department of Education (No. L2014388), the Natural Science Foundation of Liaoning Province (No. 2015020753), and Nature Science Foundation of China (No. 81503020, No. 31600767).

#### Appendix A. Supplementary data

Supplementary data related to this article can be found at <http://dx.doi.org/10.1016/j.bioactmat.2017.03.003>.

#### References

- [1] G. Kaur, N. Verma, Nature curing cancer-review on structural modification studies with natural active compounds having anti-tumor efficiency, *Bio-technol. Rep.* 6 (2015) 64–78.
- [2] L.J. Petersen, Anticoagulation therapy for prevention and treatment of venous thromboembolic events in cancer patients: a review of current guidelines, *Cancer Treat. Rev.* 35 (2009) 754–764.
- [3] P. Gupta, S.E. Wright, S.H. Kim, S.K. Srivastava, Phenethyl isothiocyanate: a comprehensive review of anti-cancer mechanisms, *BBA-Rev. Cancer* 1846 (2014) 405–424.
- [4] S. Mamidi, S. Höne, M. Kirschfink, The complement system in cancer: ambivalence between tumour destruction and promotion, *Immunobiology* 222 (2017) 45–54.
- [5] H. Izzedine, M.A. Perazella, Thrombotic microangiopathy, cancer, and cancer drugs, *Am. J. Kidney Dis.* 66 (2015) 857–868.
- [6] D. Regan, A. Guth, J. Coy, S. Dow, Cancer immunotherapy in veterinary medicine: current options and new developments, *Vet. J.* 207 (2016) 20–28.
- [7] S. Tang, Q. Meng, H. Sun, J. Su, Q. Yin, Z. Zhang, H. Yu, L. Chen, W. Gu, Y. Li, Dual pH-sensitive micelles with charge-switch for controlling cellular uptake and drug release to treat metastatic breast cancer, *Biomaterials* 114 (2017) 44–53.
- [8] D. Arora, S. Jaglan, Nanocarriers based delivery of nutraceuticals for cancer prevention and treatment: a review of recent research developments, *Trends Food Sci. Technol.* 54 (2016) 114–126.
- [9] C. Bastiancich, P. Danhier, V. Préat, F. Danhier, Anticancer drug-loaded hydrogels as drug delivery systems for the local treatment of glioblastoma, *J. Control. Release* 243 (2016) 29–42.
- [10] M. Ye, S. Kim, K. Park, Issues in long-term protein delivery using biodegradable microparticles, *J. Control. Release* 146 (2010) 241–260.
- [11] J. Cheng, Y. Jun, J. Qin, S.H. Lee, Electrospinning versus microfluidic spinning of functional fibers for biomedical applications, *Biomaterials* 114 (2017) 121–143.
- [12] X. Yang, J. Wei, D. Lei, Y. Liu, W. Wu, Appropriate density of PCL nano-fiber sheath promoted muscular remodeling of PGS/PCL grafts in arterial circulation, *Biomaterials* 88 (2016) 34–47.
- [13] J. Idaszek, E. Kijeńska, M. Łojkowski, W. Swieszkowski, How important are scaffolds and their surface properties in regenerative medicine, *Appl. Surf. Sci.* 388 (2016) 762–774.

- [14] H. Chen, Y. Liu, Q. Hu, A novel bioactive membrane by cell electrospinning, *Exp. Cell Res.* 338 (2015) 261–266.
- [15] S.F. Chou, D. Carson, K.A. Woodrow, Current strategies for sustaining drug release from electrospun nanofibers, *J. Control. Release* 220 (2015) 584–591.
- [16] C.G. Park, E. Kim, M. Park, J.H. Park, Y.B. Choy, A nanofibrous sheet-based system for linear delivery of nifedipine, *J. Control. Release* 149 (2011) 250–257.
- [17] Y. Ding, H. Hou, Y. Zhao, Z. Zhu, H. Fong, Electrospun polyimide nanofibers and their applications, *Prog. Polym. Sci.* 61 (2016) 67–103.
- [18] B. Sun, Y.Z. Long, H.D. Zhang, M.M. Li, J.L. Duvail, X.Y. Jiang, H.L. Yin, Advances in three-dimensional nanofibrous macrostructures via electrospinning, *Prog. Polym. Sci.* 39 (2014) 862–890.
- [19] J. Ko, D. Kan, M.B.G. Jun, Combining melt electrospinning and particulate leaching for fabrication of porous microfibers, *Manuf. Lett.* 3 (2015) 5–8.
- [20] X. Li, H. Liu, J. Wang, C. Li, Preparation and characterization of poly( $\epsilon$ -caprolactone) nonwoven mats via melt electrospinning, *Polymer* 53 (2012) 248–253.
- [21] M.V. Natu, H.C. de Sousa, M.H. Gil, Influence of polymer processing technique on long term degradation of poly( $\epsilon$ -caprolactone) constructs, *Polym. Degrad. Stabil.* 98 (2013) 44–51.
- [22] C.C. Qin, X.P. Duan, L. Wang, L.H. Zhang, M. Yu, R.H. Dong, X. Yan, H.W. He, Y.Z. Long, Melt electrospinning of poly(lactic acid) and polycaprolactone microfibers by a hand-operated Wimshurst generator, *Nanoscale* 7 (2015) 16611–16615.
- [23] E. Zhmayev, D. Cho, Y.L. Joo, Modeling of melt electrospinning for semi-crystalline polymers, *Polymer* 51 (2010) 274–290.
- [24] T. Elzein, M. Nasser-Eddine, C. Delaite, S. Bistac, P. Dumas, FTIR study of polycaprolactone chain organization at interfaces, *J. Colloid Interf. Sci.* 273 (2004) 381–387.
- [25] M. Simeonova, G. Ivanova, V. Enchev, N. Markova, M. Kamburov, C. Petkov, A. Devery, R. O'Connor, D. Brougham, Physicochemical characterization and *in vitro* behaviour of daunorubicin-loaded poly(butylcyanoacrylate) nanoparticles, *Acta Biomater.* 5 (2009) 2109–2121.
- [26] J. Lyons, C. Li, F. Ko, Melt-electrospinning part I: processing parameters and geometric properties, *Polymer* 45 (2004) 7597–7603.
- [27] T.D. Brown, P.D. Dalton, D.W. Hutmacher, Melt electrospinning today: an opportune time for an emerging polymer process, *Prog. Polym. Sci.* 56 (2016) 116–166.